TOP2B Enzymatic Activity on Promoters and Introns Modulates Multiple Oncogenes in Human Gliomas

Edgar Gonzalez-Buendia[1], Junfei Zhao[2], Lu Wang[3], Subhas Mukherjee[4], Daniel Zhang[1], Víctor A. Arrieta[1,5], Eric Feldstein[1], J. Robert Kane[1], Seong Jae Kang[1], Catalina Lee-Chang[1], Aayushi Mahajan[6], Li Chen[1], Ronald Realubit[7], Charles Karan[7], Lisa Magnuson[1], Craig Horbinski[1,4], Stacy A. Marshall[3], Jann N. Sarkaria[8], Ahmed Mohyeldin[9], Ichiro Nakano[10], Mukesh Bansal[2], Charles D. James[1], Daniel J. Brat[4], Atique Ahmed[1], Peter Canoll[6], Raul Rabadan[2], Ali Shilatifard[3], and Adam M. Sonabend[1]

ABSTRACT

Purpose: The epigenetic mechanisms involved in transcriptional regulation leading to malignant phenotype in gliomas remains poorly understood. Topoisomerase IIB (TOP2B), an enzyme that decoils and releases torsional forces in DNA, is overexpressed in a subset of gliomas. Therefore, we investigated its role in epigenetic regulation in these tumors.

Experimental Design: To investigate the role of TOP2B in epigenetic regulation in gliomas, we performed paired chromatin immunoprecipitation sequencing for TOP2B and RNA-sequencing analysis of glioma cell lines with and without TOP2B inhibition and in human glioma specimens. These experiments were complemented with assay for transposase-accessible chromatin using sequencing, gene silencing, and mouse xenograft experiments to investigate the function of TOP2B and its role in glioma phenotypes.

Results: We discovered that TOP2B modulates transcription of multiple oncogenes in human gliomas. TOP2B regulated transcription only at sites where it was enzymatically active, but not at all native binding sites. In particular, TOP2B activity localized in enhancers, promoters, and introns of PDGFRA and MYC, facilitating their expression. TOP2B levels and genomic localization was associated with *PDGFRA* and *MYC* expression across glioma specimens, which was not seen in nontumoral human brain tissue. *In vivo*, TOP2B knockdown of human glioma intracranial implants prolonged survival and downregulated *PDGFRA*.

Conclusions: Our results indicate that TOP2B activity exerts a pleiotropic role in transcriptional regulation of oncogenes in a subset of gliomas promoting a proliferative phenotype.

[1]Department of Neurosurgery, Feinberg School of Medicine, Northwestern University and Northwestern Medicine Malnati Brain Tumor Institute of the Robert H. Lurie Comprehensive Cancer Center, Feinberg School of Medicine, Northwestern University, Chicago, Illinois. [2]Department of Systems Biology, Herbert Irving Comprehensive Cancer Center, Columbia University, New York, New York. [3]Department of Biochemistry and Molecular Genetics, Feinberg School of Medicine, Northwestern University, Chicago, Illinois. [4]Department of Pathology, Feinberg School of Medicine, Northwestern University, Chicago, Illinois. [5]PECEM, Facultad de Medicina, Universidad Nacional Autónoma de México, México. [6]Department of Pathology and Cell Biology, Columbia University, New York, New York. [7]High-Throughput Screening Genome Center, Columbia University, New York, New York. [8]Department of Radiation Oncology, Mayo Clinic, Rochester, Minnesota. [9]Department of Neurosurgery, Ohio State University, Columbus, Ohio. [10]Department of Neurosurgery, University of Alabama, Birmingham, Alabama.

Introduction

Gliomas, the most common of all primary brain tumors in adults, are notable for their remarkable molecular heterogeneity. Glioblastoma (GBM) diagnosis is defined by histologic appearance, yet within this diagnosis there is a broad spectrum of tumor phenotypes and molecular characteristics. With respect to the latter, GBM have been classified by patterns of gene expression that are clinically and biologically meaningful (1, 2). However, the mechanisms responsible for these transcriptional signatures are not well understood.

Epigenetic mechanisms responsible for specific gene expression patterns can be a consequence of gene mutations. For instance, *IDH1/2* mutations lead to global DNA methylation patterns that have effects on chromatin organization (3–6). Another such example involves the mutation of histone genes that alter the pattern of posttranslational modification of wild-type histones, which also has global transcriptional consequences (7, 8). Yet the majority of adult GBM do not have these mutations, and consequently the epigenetic basis for the variable expression patterns observed on most adult GBM has not been elucidated.

Topoisomerase 2 (TOP2) have been shown to de-coil chromatin through transient double-strand DNA breaks (DSB), releasing torsional forces and enhancing DNA accessibility for RNA polymerases and transcription factors (9, 10). TOP2 contributes to chromatin organization and the spatial architecture in the nucleus through matrix attached regions (MARs)/scaffold associated regions (SAR; refs. 11, 12) and topological associated domains (TAD) that play a role in the gene expression regulation and maintenance of genome architecture (13, 14).

Translational Relevance

Glioblastomas are notorious for their molecular heterogeneity, a feature that challenges prediction of individual response to therapy. Whereas some gliomas harbor IDH1/2 and H3K27 mutations that modulate chromatin structure and associated cancer phenotype, the epigenetic basis for variable oncogene expression of 90% of glioblastomas, which do not contain these mutations, remains elusive. We discovered that TOP2B exerts pleiotropic modulation of multiple oncogenes in a subset of gliomas. Our results support a model of TOP2B transcriptional regulation that is not primarily associated with maintaining of chromatin accessibility by this topoisomerase.

TOP2A and TOP2B, the two isoforms of TOP2, differ in their expression and cellular functions (15). In development, TOP2A is typically expressed by cycling cells, whereas TOP2B is primarily expressed by post-mitotic cells (9, 10). TOP2A has been implicated in the regulation of transcription in stem cells (9), and plays a role in DNA repair, transcription, and chromosome segregation (16). TOP2B has been shown to drive the neuronal differentiation during development (9, 17), and is required for transcription of early response genes following depolarization of mature neurons (18). TOP2B is involved in the expression of long genes in these cells (19). Moreover, TOP2B has been implicated in DSB leading to genome fragility and translocations in cancer (13, 20, 21).

We hypothesized that TOP2B plays a role in the regulation of key oncogenic drivers in a subset of gliomas. In this study, we investigated the transcriptional consequences of TOP2B expression, genomic binding, and enzymatic activity in gliomas. In so doing, we have discovered that this enzyme regulates the expression of multiple genes, several of which have known oncogenic activity. As a way of example of oncogene modulation by TOP2B, we show that *PDGFRA* and *MYC* expression is influenced by TOP2B enzymatic activity on these gene loci in these tumors.

Materials and Methods

Cell culture

TS543 *PDGFRA*[Amp] human glioma cell line was kindly provided by Dr. Brenan (Memorial Sloan Kettering Cancer Center, New York, NY) and has been described previously (22). It was cultured with Neurocult (NS Basal medium) complemented with Neurocult human supplemented (NS human), antibiotics 1×, supplemented with EGFR, FGF, and heparin. BT142 *IDH1*[R132H] cell line was obtained from ATCC and confirmed identity by short tandem repeat (STR), cultured with Neurocult (NS Basal medium) complemented with Neurocult human supplemented (NS human), antibiotics 1×, supplemented with EGFR, FGF, heparin, and PDGF-AA. SNB19 has been described before and confirmed by STR, was cultured with MEM, FBS 10%, MEM nonessential amino acids, sodium pyruvate, L-glutamine, and antibiotics 1×. 0777A human glioma cell line was generated by Dr. Ichiro Nagano, University of Alabama at Birmingham (Birmingham, AL) and cultured in laminin-coated dishes with DMEM/F12 medium, B27, antibiotics, and FGF, EGF, and heparin. Cells were cultured 37°C and 5% CO_2. TS543, BT142, SNB19, and 0777A cells were PCR tested for *Mycoplasma* (ATCC, 30–1012K) and, profiled by STR for reproducibility and maintaining control of their identity. Whereas no previous

STR profiles were available for TS543 and 0777A, BT142, and SNB19 had 100% match with the known STR profile for these lines.

Decatenation assay

Decatenation assay was performed as follows: nuclear extracts were isolated using Buffer N1 containing Tris-HCl 15 mmol/L pH 7.5, sucrose 300 mmol/L, HEPES 10 mmol/L, KCl 60 mmol/L, $MgCl_2$ 4 mmol/L, DTT 1 mmol/L, NaCl 5 mmol/L, incubated 10 minutes with Cell lysis buffer N1, Igepal 0.1%, Triton X-100 1%. Nuclear extract was incubated in a decatenation reaction using Topoisomerase II assay kit (TopoGEN catalog No. TG1001–1) and the products were analyzed on agarose gel 1%.

Assay for transposase-accessible chromatin using sequencing

We used assay for transposase-accessible chromatin using sequencing (ATAC-seq) method as reported previously (ref. 23; relevant controls on Supplementary Fig. S11). Cells were treated with TOP2 inhibitor ICRF-193 10 µmol/L for 6 hours or DMSO. Data were analyzed using the bio-atac platform Buenrostro lab.

Chromatin immunoprecipitation sequencing

For chromatin immunoprecipitation sequencing (ChIP-seq) and native ChIP-seq of TOP2B, 5×10^7 cells were treated with etoposide (0.5 mmol/L), for 10 minutes, or DMSO as reported previously (24), crosslinked using formaldehyde 1% (FA1%) or non-FA1% as indicated. Nuclear extracts were isolated, and chromatin was fragmented using Covaris sonicator. Ten micrograms of antibody (TOP2B Abcam ab72334; Abcam H3K4me1 ab8895, H3K4me2 ab32356, H3K4me3 ab8580, H3K27Ac ab4729, H3K27me3 ab6002, H3K9me3 ab8898, H3K36me3 ab9050), was incubated overnight (relevant controls on Supplementary Fig. S11). Washes were performed with RIPA Buffer four times followed by a final wash of TE 50 mmol/L NaCl. The crosslink was reversed and DNA was purified using phenol:chloroform:isoamyl alcohol for library preparation and sequencing. To analyze ChIP-seq data, we used MACS2 peak calling (Supplementary Table S2). We used Fisher exact test to calculate significance relative to random regions of the genome of size similar to the peaks from TOP2B.

cDNA

Total RNA was extracted from indicated cells with Direct-zol RNA MiniPrep Plus (Zymo Research) according to the manufacturer's instructions, and treated with DNaseI (Promega). cDNA was generated from 1 µg DNaseI-treated RNA (Reverse Transcription System, Promega). followed by qPCR amplification. The relative expression levels of gene expression were determined by using *GAPDH* mRNA levels as an endogenous reference, and the $\Delta\Delta C_t$ method was used for normalization.

RNA-sequencing

Total RNA was extracted from indicated cells with Direct-zol RNA MiniPrep Plus (Zymo Research) according to the manufacturer's instructions and sequenced. RNA sequencing (RNA-seq) data were used for gene set enrichments for TOP2B and analyzed with Bioconductor platform for differential expression analysis.

Western blot analysis

Western blot analysis was used to evaluate protein abundance. The following antibodies were used: TOP2B (Abcam, ab72334), PDGFRA (Cell Signaling Technology, 5241S), MYC (Cell Signaling Technology, 9402S) GAPDH (Santa Cruz Biotechnology, sc365062), H3 (pan-Histone3, Cell Signaling Technology, 4620S).

TOP2 inhibition

Cells were treated at 37°C with ICRF-193 10 μmol/L for 6 hours (RNA) and 48 hours (protein). Top2 inhibition was confirmed by decatenation assays (TOPOKIT). Total RNA was extracted followed by RNA-seq. A *t* test showing $P < 0.05$ or Pearson $P < 0.05$ was considered significant, and DE-seq adjusted $P < 0.05$ was defined as significant for RNA-seq data.

Statistical analysis

Enrichment of TOP2B binding in promoter or intron were evaluated using Fisher exact test implemented in bedtools (25). The two-sided *t* test was generally used to compare two populations.

Animal studies

All animal studies were performed in accordance with Northwestern's Institutional Animal Care and Usage Committee. Mice were housed in pathogen free conditions in a relatively constant temperature of 24°C and humidity of 30% to 50%. Six- to 8-week-old male and female athymic nude mice purchased from Charles River Laboratories were used in these studies.

In vivo TET-ON–inducible TOP2B knockdown in intracranial xenograft mouse model

Mice were anesthetized with K/X cocktail and checked for deepness of anesthesia via paw pinch method. Once proper depth of anesthesia was observed, a 1-cm incision was made in the midline of the mouse head to expose the skull underneath. A transcranial burr hole was created using sterile hand-held drill and mouse was mounted on a stereotaxic device. 2×105 BT142 glioma cells in 2.5 μL of sterile PBS were loaded into a 29G Hamilton Syringe and injected slowly over a period of 3 minutes into the left hemisphere of the mouse brain at 3-mm depth through the transcranial burr hole created 3 mm lateral and 2 mm caudal relative to bregma and midline sutures. Following injection, incision was closed using 9-mm stainless steel wound clips and mouse was placed into a clean cage placed onto a heating pad until recovery from anesthesia.

Mice injected with TET-ON–inducible TOP2B shRNA BT142 clones were fed access to 0.35% (w/v) doxycycline in 5% sucrose water starting two days after intracranial injection. Control mice were fed 5% sucrose water only. Mice were euthanized upon visible signs of tumor burden such as >20% weight loss, hunched posture, and other neurologic symptoms. Upon euthanasia, brains were harvested and imaged with Nikon AZ100 epi-fluorescent microscope (ex/em 565/620, exposure time 2 seconds).

IHC

IHC was performed as previously described (26). We used MYC (Abcam, ab32072), PDGFRA (Cell Signaling Technology, 5241) and TOP2B (Abcam, ab72334) antibodies. Counterstaining was done with hematoxylin and eosin. Images were acquired using a light microscope with camera (Leica DM2000 LED, Leica DFC450 C, Leica Microsystems). Human specimens or mouse tumor slides were scanned using the NanoZoomer 2.0-HT slide scanner (Hamamatsu Photonics) and visualized with the NDP.view2 Viewing software. HistoQuest version 6.0 software (TissueGnostics) was used to quantify the MYC-, PDGFRA-, or TOP2B-positive cells per total cell number or mm^2 as indicated in the figure legend. Parameters were adjusted to detect nuclei first by hematoxylin staining. We applied a threshold to the mean intensity of DAB chromogen for all the cells to define positive staining nuclei for MYC and TOP2B. To quantify PDGFRA, having identified cells by hematoxylin staining, each of these cells underwent segmentation of nuclear and cytoplasmic compartments. Then, the cytoplasmic PDGFRA staining was quantified after applying a threshold to the mean intensity of the DAB chromogen for all cells. The same thresholds and parameters were used for all tumor samples.

Immunofluorescence staining

BT142 *IDH*[R132H] glioma cells were treated with ICRF-193, 10 μmol/L for 6 hours. The cells were stained after. Briefly, cells were fixed with 4% paraformaldehyde and then permeabilized with 0.5% Triton X-100 in $1\times$ PBS. The primary antibody was incubated overnight at 4°C. Anti-γH2A.X (phospho S139) antibody (Abcam ab22551).

Microscopy

The slides were visualized using the Nikon A1R confocal microscope at the Nikon Imaging center at the Northwestern University (Chicago, IL).

Immuno dot blot

We used Recombinant Anti-5-methylcytosine (5-mC) antibody (Abcam ab214727) to quantify global DNA methylation levels. BT142 *IDH1*[R132H] glioma cells treated with ICRF-193 10 μmol/L for 6 hours and DMSO as a control were pelleted for genomic DNA extractions. Serial dilutions 100 ng, 50 ng, and 25 ng were blotted in nitrocellulose membrane.

Data availability

The ChIP-seq for cell lines and human specimens ChIP-seq, RNA-seq and ATAC-seq data that support the findings of this study are available on GEO, accession number GSE133561.

Results

TOP2B localizes to sites with accessible chromatin and active transcription

Previous groups have shown that only a subset of TOP2A/B–binding sites are subject to transcriptional regulation by TOP2A/B activity (9, 10). On the other hand, in neurons, TOP2B is poised at specific loci, and only induces DNA breaks and facilitates transcription following depolarization (18). Thus, it appears that TOP2B-related transcriptional regulation is modulated by its activity at particular sites, and conversely, TOP2B is not active in all sites where it is localized. We hypothesized that identifying sites of TOP2B activity, rather than all sites of TOP2B DNA binding, would reveal genes whose expression is regulated by this enzyme. To this end, we performed ChIP-seq experiments in two conditions: (i) using glioma cells treated with DMSO only to identify loci associated with TOP2B recruitment (native binding); and (ii) treating the cells with etoposide for 10 minutes, to trap TOP2B at sites where it is enzymatically active. Etoposide is a poison that stalls the enzymatic reaction of TOP2A/B following DSB induction by this enzyme, and stabilizes the TOP2–DNA complexes through a covalent bound (27, 28). Previous groups have performed TOP2 ChIP-seq in the setting of etoposide for 10 minutes as a means of stabilizing TOP2–chromatin interactions (24, 29). With this approach, we identified distinct sites for TOP2B native binding and enzymatic activity, which were variable across the glioma cell lines and human specimens analyzed (**Fig. 1A**). To investigate whether the TOP2B peaks encountered in the setting of etoposide-ChIP were related to nonspecific signal related to formaldehyde-cross linking, we compared the TOP2B activity peaks by performing TOP2B etoposide-ChIP in the presence versus absence
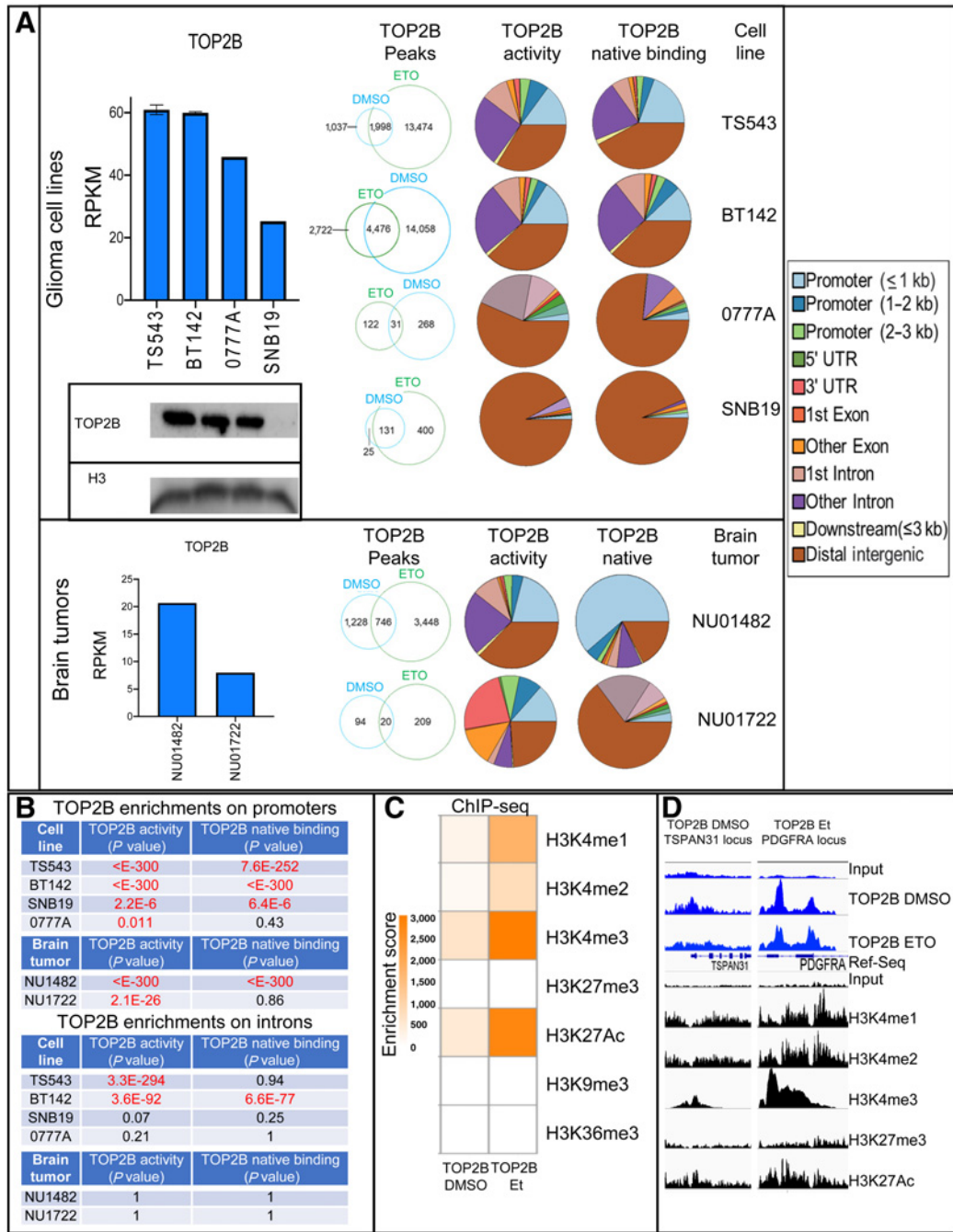
Figure 1.
A, TOP2B expression determined by RNA-seq (TS543 DMSO 10 replicates, BT142 DMSO five experimental replicates, 0777A one experimental replicate, SNB19 1 experimental replicate) and Western blot on human glioma cell lines (two independent experiments on TS543, BT142, 0777A, SNB19) and human glioma specimens (NU01482, NU01722; left). Genome-wide distribution of TOP2B native binding and activity peaks determined by DMSO and etoposide (Et) ChIP-seq in different glioma cell lines were performed (top-center panel; TS543 two DMSO/etoposide experimental replicates, BT142 two DMSO/etoposide experimental replicates, 0777A 1 DMSO/etoposide experiment, SNB19 2 DMSO/etoposide experiments) and human glioma tumors (bottom-center panel; NU01482 1 DMSO/etoposide experimental replicate, NU01722 1 DMSO/etoposide experimental replicate). **B,** Table containing enrichment P values of TOP2B peaks for promoter and intron regions relative to random regions in the genome (Fisher exact test). **C,** Heatmap illustrating colocalization of histone marks with TOP2B native binding and activity peaks determined by histone marks (Fisher exact test). **D,** Examples of histone marks at genomic regions with TOP2B native binding (TOP2B DMSO ChIP) and TOP2B enzymatic activity (TOP2B etoposide ChIP). Same y-axis scale was used for input and for the corresponding ChIP track.

of formaldehyde cross-linking. Interestingly, this analysis revealed that the localization TOP2B activity determined by etoposide-ChIP was independent of the formaldehyde-cross linking process (Supplementary Fig. S1).

TOP2B activity peaks were over-represented in the promoters of all cell lines and clinical glioma specimens examined, and localization of TOP2B native binding was over-represented in promoter regions of three of four human glioma cell lines and a representative human glioma sample examined (**Fig. 1B**). Surprisingly, overrepresentation of intron activity sites was observed for cell lines TS543 and BT142, but not in other samples. BT142 cells also showed overrepresentation of TOP2B native binding at intron locations (**Fig. 1B**). Together, these results show that TOP2B is enriched in promoters and introns. TOP2B native genome binding and TOP2B activity is variable across gliomas, and whereas there is overlap between binding and activity, there are also sites that are uniquely captured with DMSO versus etoposide ChIP conditions.

We investigated the histone modification status at sites of TOP2B localization. Genome-wide analysis of ChIP-seq on TS543 glioma cells showed that both TOP2B native binding and activity sites coincided with histone modifications characteristic of open/accessible chromatin, including H3K4me1, H3K4me2, H3K4me3, and H3K27Ac, but not with marks of heterochromatin such as H3K27me3 or H3K9me3 (Fisher exact test, **Fig. 1C**). H3K4me3 and H3K27Ac histone marks showed stronger cooccurrence with TOP2B activity sites compared with TOP2B native binding (Fisher exact test, **Fig. 1C** and **D**).

TOP2B activity in promoters and introns regulates gene expression

The enrichment of TOP2B native binding and activity in promoters and introns, as well as the colocalization of this topoisomerase with sites marked by H3K4me3 and H3K27Ac suggests that the majority of TOP2B–genome interactions in gliomas relate to transcription. Interestingly, whereas we observed an overlap of genes with TOP2B localization in promoters across samples analyzed, we also identified genes that had TOP2B promoter localization only in one of the samples (Supplementary Fig. S2). We investigated whether TOP2B localization in promoters was related to baseline gene expression, to determine whether genes with highest baseline expression on a given cell line are those that have TOP2B in promoters. Gene set enrichment analysis (GSEA) did not show a direct correlation between baseline gene expression determined by RNA-seq and TOP2B native binding or activity in promoters in TS543 (Supplementary Fig. S3). Together, these findings suggest that TOP2B promoter localization is seen in a specific group of genes, which is variable across glioma cell lines.

To investigate the functional implications of TOP2B binding and/or activity at gene promoters, we evaluated gene expression by RNA-seq following pharmacologic TOP2 inhibition with ICRF-193, and confirmed TOP2 inhibition with this drug concentration by a decatenation assay as previously done (ref. 30; Supplementary Fig. S4). In cell line BT142, gene-set variation analysis (GSVA) showed that as a group, genes with TOP2B etoposide ChIP peaks in promoters were significantly downregulated following TOP2 inhibition with ICRF-193 relative to other genes (**Fig. 2A**). Downregulation of genes included those loci with TOP2B activity only and those in which a coincidence of TOP2B activity and native binding was observed (**Fig. 2B**). In contrast, genes that only had TOP2B native binding, but no TOP2B activity peaks, did not show expression changes following TOP2 inhibition (**Fig. 2A** and **B**). Similar findings were observed following

ICRF-193 treatment of cell line TS543 (Supplementary Fig. S5). Similar results were obtained when GSEA was used for these analyses.

Previous groups described that TOP2B releases torsional forces and leads to increased chromatin accessibility (decrease in histone density) as a mechanism that facilitates transcription (9, 10, 13, 31). Thus, we investigated whether TOP2B inhibition led to changes in chromatin accessibility determined by ATAC-seq at the promoters where it localized. Surprisingly, these results revealed no consistent change in chromatin accessibility at promoter sites containing TOP2B binding or activity of genes that suffered downregulation following TOP2 inhibition (Supplementary Fig. S5), as some downregulated genes suffered decrease in chromatin accessibility, whereas other genes that were also downregulated increased accessibility in response to TOP2 inhibition. TOP2 inhibition with ICRF-193 for 6 hours also had no effect on H3K4me3 and H3K27Ac marks determined by ChIP-seq (Supplementary Fig. S5). As expected, sites with H3K4me3 or H3K27Ac modifications were associated with accessible chromatin, validating that open chromatin was identified with the same ATAC-seq experiment that did not reveal changes in chromatin accessibility following TOP2 inhibition (Supplementary Fig. S5). Together, these findings support that in this context, TOP2B modulation of gene expression in gliomas is related to its enzymatic activity at corresponding promoters, but independent of chromatin accessibility as well as H3K4me3 or H3K27Ac histone modifications at these sites.

Given the observed enrichment of TOP2B DMSO and etoposide ChIP peaks in introns, we investigated whether TOP2B enzymatic activity modulates gene expression at these sites.

Similar to results associated with promoter localization, the groups of genes with TOP2B activity in introns exhibited significant downregulation following TOP2 inhibition by ICRF-193. As opposed to the case of promoters, genes with TOP2B native binding in introns also exhibited downregulation following TOP2B inhibition treatment, yet this effect was modest compared with the downregulation observed for genes that had TOP2B activity in introns determined by TOP2B etoposide ChIP (**Fig. 2C** and **D**). GSEA analysis revealed a strong correlation between gene length and presence of TOP2B intron localization in TS543 and BT142 cell lines ($P < 0.001$), consistent with a previous report that TOP2B facilitates expression of long genes (19).

To explore what might be the transcription factors associated with TOP2B in gliomas, we performed multiple motif enrichment analysis using the ChIP-seq peaks in the glioma cell lines (Supplementary Fig. S6). We found that CTCF is the most common motif in both TOP2B native and active peaks, consistent with previous studies (14).

TOP2B modulates *PDGFRA* and *MYC* oncogenes in glioma cell lines

PDGFRA and *MYC* were among the genes with TOP2B localization that suffered most significant downregulation following ICRF-193 treatment on glioma cells (**Fig. 3A–D**). Moreover, MYC targets were among the gene signatures that were downregulated by TOP2B inhibition the most on an unbiased analysis using a larger compendium of gene sets (refs. 32, 33; MSigDB gene lists; Supplementary Table S1). In TS543, MYC targets were the most significant downregulated gene set upon TOP2B inhibition ($P_{adj} < 1.4E\text{-}08$), and on BT142 these were also significantly downregulated ($P_{adj} < 6.56E\text{-}04$; Supplementary Table S1). TOP2B coincided with H3K4me3 as well as H3K27Ac in the promoter and gene body of both *PDGFRA* and *MYC* (**Fig. 3A–D**). Moreover, TOP2B native binding and activity also localized at a locus previously reported as a *MYC* enhancer (34), where
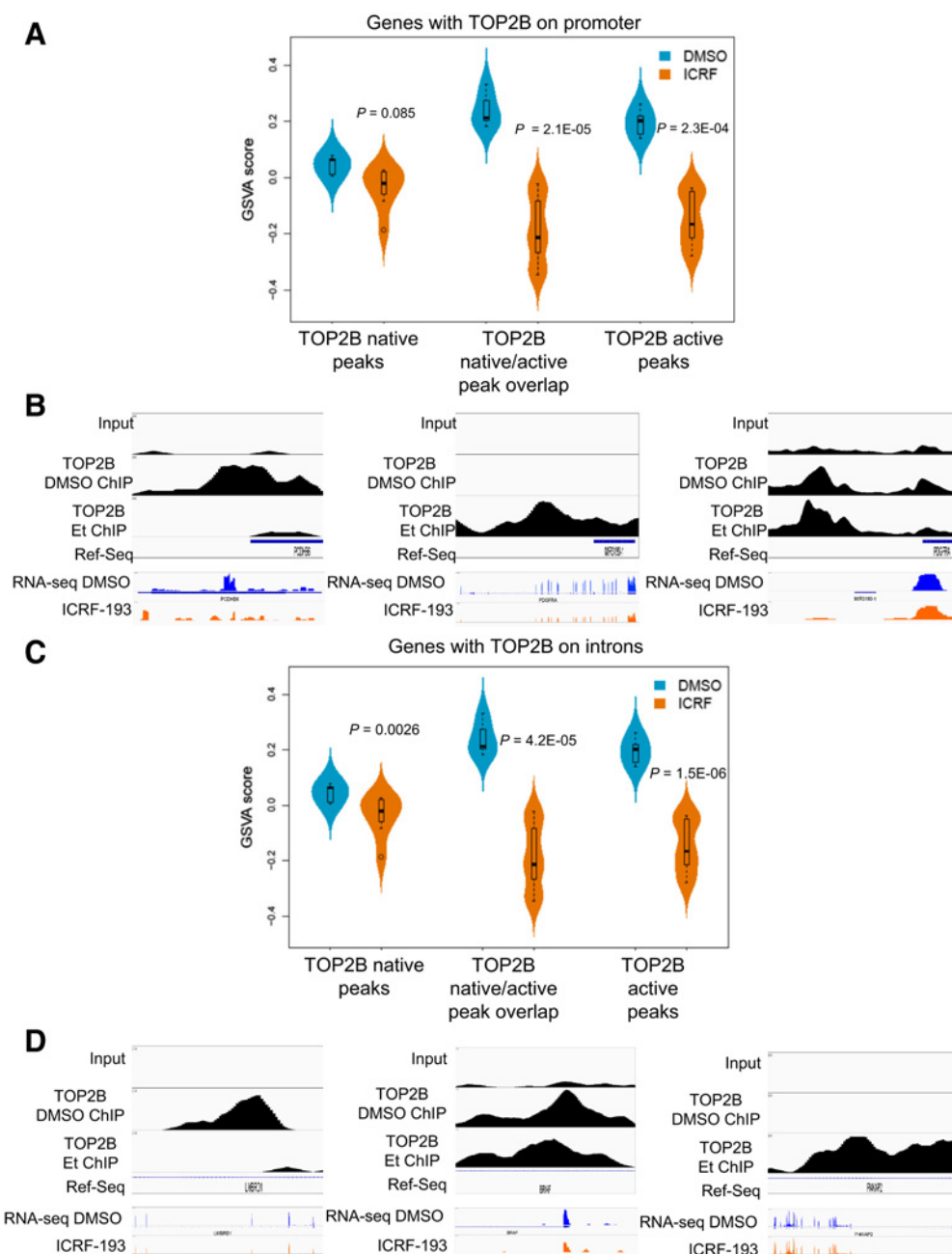
Figure 2.

The activity of TOP2B on promoter and introns regulates gene expression in BT142 glioma cell line. **A,** GSVA plot of gene expression [RNA-seq DMSO (five experimental replicates) and ICRF-193 in seven experimental replicates] with TOP2 inhibition at promoters with TOP2B peaks detected by DMSO ChIP only, TOP2B peaks detected by DMSO and etoposide (Et) ChIP, and TOP2B peaks only detected etoposide ChIP only. **B,** Examples of ChIP-seq data and RNA-seq at promoter sites. **C,** GSVA analysis of effect of TOP2 inhibition on genes with TOP2B native binding and/or activity on introns (presented similar to **A**). **D,** Examples of ChIP-seq data and RNA-seq at intron sites. For **B** and **D**, the y-scale is maintained constant for all tracks within a specific locus.

it coincided with H3K4me1 (**Fig. 3B**). Using a doxycycline-based inducible shRNA system, we observed that TOP2B silencing in BT142 cells led to a decrease in PDGFRA and MYC protein levels (**Fig. 3E**). We also observed downregulation of MYC transcriptional targets following ICRF-193 treatment (TS543 $P = 1.7E-07$ and BT142 $P = 0.00087$, **Fig. 3F**).

Given that *PDGFRA* is amplified in 15% of GBM (35), we investigated whether amplification of this gene was associated with downregulation following TOP2 inhibition. We analyzed copy number for *PDGFRA* by qPCR and found that this gene is only amplified in TS543, but not on BT142 or SNB19 (Supplementary Fig. S7). The elevated expression of *PDGFRA* on BT142 relates to
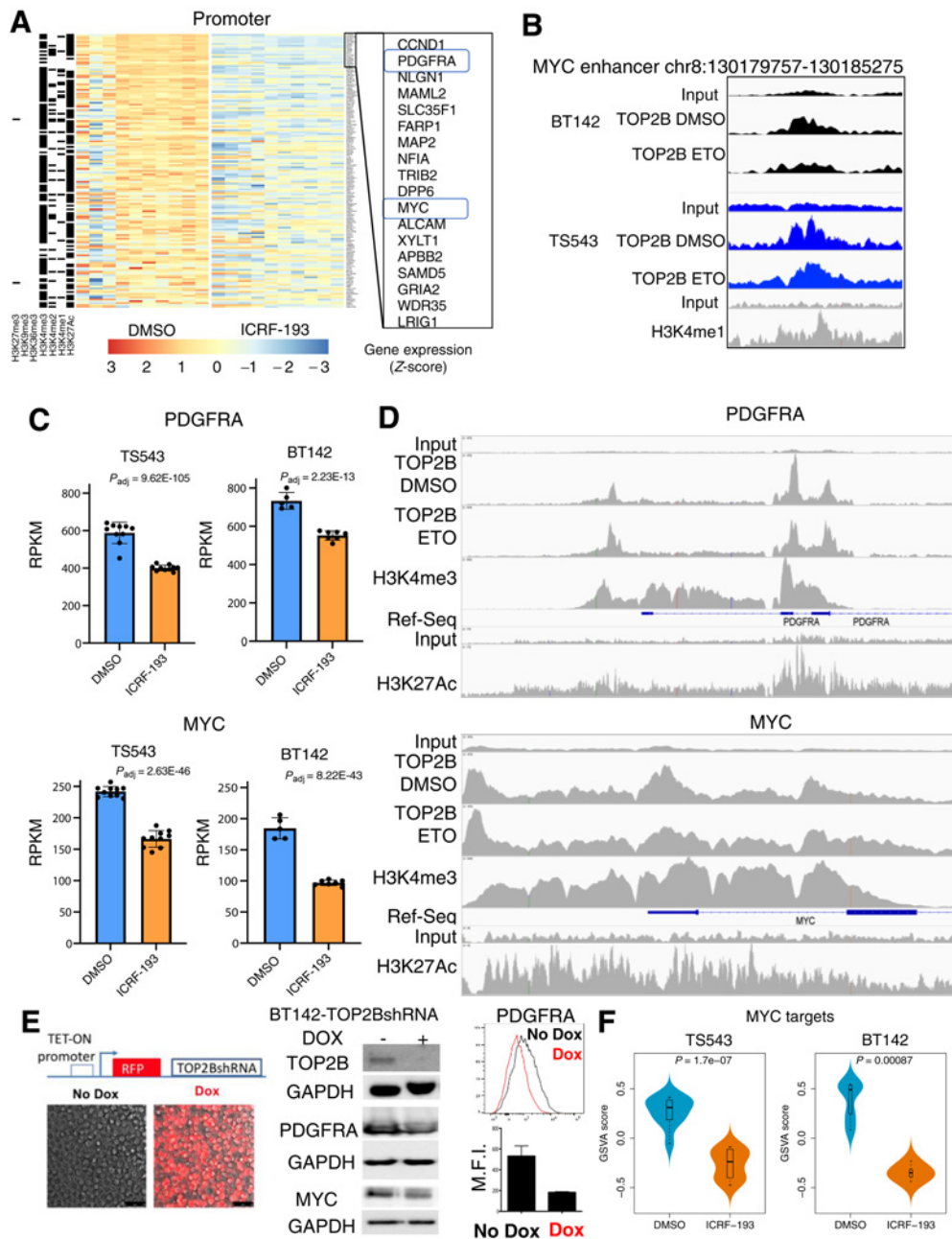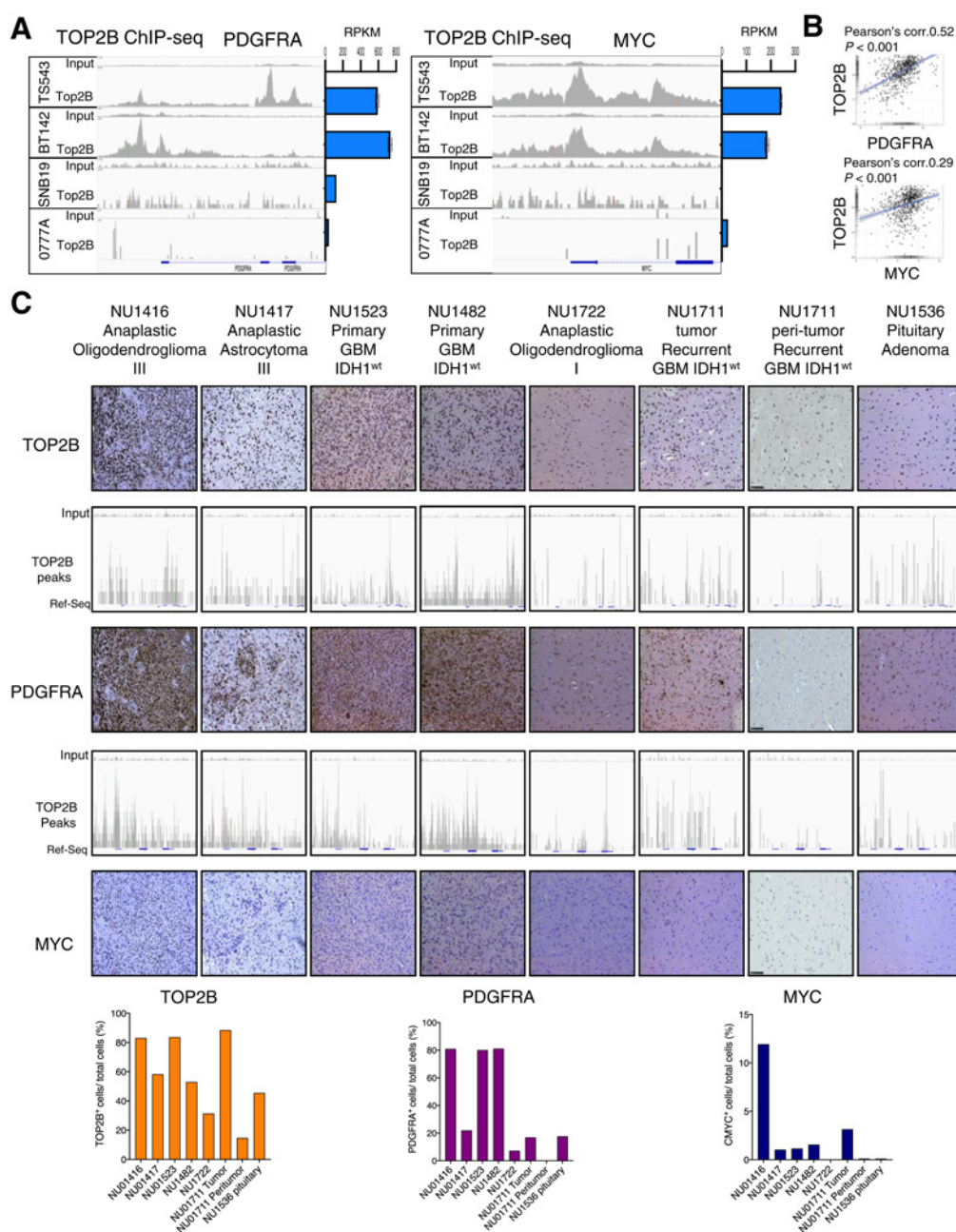
Figure 3.
TOP2B modulates transcription of *PDGFRA* and *MYC* in gliomas. **A,** Heatmap showing gene expression changes following ICRF-193 treatment for genes with TOP2B activity [etoposide (Et) ChIP] on promoters in TS543 (genes are sorted by most significant to less significant downregulation by ICRF-193 in descending order and each column represent one experimental replicate, 10 in total). **B,** Tracks of DMSO and Et ChIP by duplicate for TOP2B and H3K4me1 in TS543 and BT142 at *MYC* enhancer region reported by Herranz and colleagues. **C,** Expression of *PDGFRA* and *MYC* in TS543 (DMSO 10 experimental replicates, ICRF-193 10 experimental replicates) and BT-142 (DMSO five experimental replicates, seven ICRF-193 experimental replicates) cell line following TOP2 inhibition with ICRF-193 determined by RNA-seq. **D,** TS543 tracks of DMSO and etoposide ChIP for TOP2B as well as histone marks H3K4me3 and H3K27Ac at *PDGFRA* (top) and *MYC* locus (bottom). For these, track *y*-axis was equally scaled for input (top), TOP2B and H3K4me3. A separate and equal scale was used H3K27Ac and corresponding input as reference (bottom). **E,** Protein levels of PDGFRA and MYC following shRNA-based TOP2B silencing in a TET-ON system on BT142, determined by WB and FACS (for PDGFRA) and WB (for MYC). For **E,** three experiments with three replicates were performed. **F,** GSVA for MYC targets (RNA-seq) following 6 hours of TOP2 inhibition in TS543 (DMSO and ICRF-193 10 experimental replicates) and BT142 (five DMSO and ICRF-193 seven experimental replicates) cell lines.

Figure 4.
TOP2B expression and genomic localization at *PDGFRA* and *MYC* loci is associated with the expression of these genes in human gliomas. **A,** ChIP-seq for TOP2B native binding (DMSO ChIP; left) and RNA-seq data (right) shows genomic binding and expression of *PDGFRA* (left) and *MYC* (right) across human glioma cell lines. ChIP-seq tracks presented are representative of the following experimental replicates: TS543 (*n* = 2), BT142 (*n* = 2), 0777A (*n* = 1), and SNB19 (*n* = 2). **B,** Correlation of expression between *TOP2B* versus *PDGFRA* mRNA (top) and *TOP2B* vs. *MYC* mRNA (bottom) in human gliomas (including low-grade gliomas and GBM) from TCGA GlioVis portal http://gliovis.bioinfo.cnio.es/) determined by Pearson coefficient. **C,** ChIP-seq for TOP2B at the *PDGFRA* and *MYC* loci performed in a set of different glioma human specimens and a sample of peritumoral brain, as well as a pituitary adenoma paired with expression of these proteins determined by IHC (top), and is respective quantification shown in bar plots (bottom). Expression of these proteins were determined by IHC. The slides were quantified for the positive cells and normalized per total cell number for TOP2B, PDGFRA and MYC using HistoQuest version 6.0 software (TissueGnostics). Same *y*-axis scale was used for input and for the corresponding ChIP track in all cases.

aberrant promoter–enhancer interactions previously described (3). Thus, these results indicate that the modulation of *PDGFRA* expression by TOP2B is independent of the amplification status of this oncogene.

TOP2B genomic localization at *PDGFRA* and *MYC* is associated with their expression in gliomas

TOP2B native binding and activity peaks at *PDGFRA* and *MYC* loci were associated with the baseline expression of these genes

across four glioma cell lines (**Fig. 4A**). We also observed a correlation between TOP2B and *PDGFRA* expression, as well as a modest correlation between TOP2B with *MYC* mRNA expression through analysis of TCGA GBM data (**Fig. 4B**). These results prompted our analysis of TOP2B expression and genomic binding at *PDGFRA* and *MYC* loci in human glioma specimens. We stained eight patient tumors/samples for TOP2B, PDGFRA, and MYC, including glioma tissues, peritumoral brain, as well as a pituitary adenoma, and ranked these according to IHC staining intensity. This analysis revealed that elevated PDGFRA and MYC was associated with

TOP2B peaks at these gene loci across human gliomas and non-glioma specimens (**Fig. 4C**).

TOP2B expression is associated with tumor growth in gliomas

Given the effects of TOP2B in the transcription of *PDGFRA* and *MYC*, key drivers of glioma tumor biology, we investigated the phenotype associated with the expression of this topoisomerase. GSVA transcriptional analysis of GBM revealed that tumors with high TOP2B levels are associated with elevated expression of cell cycle–related genes when compared with tumors with low TOP2B
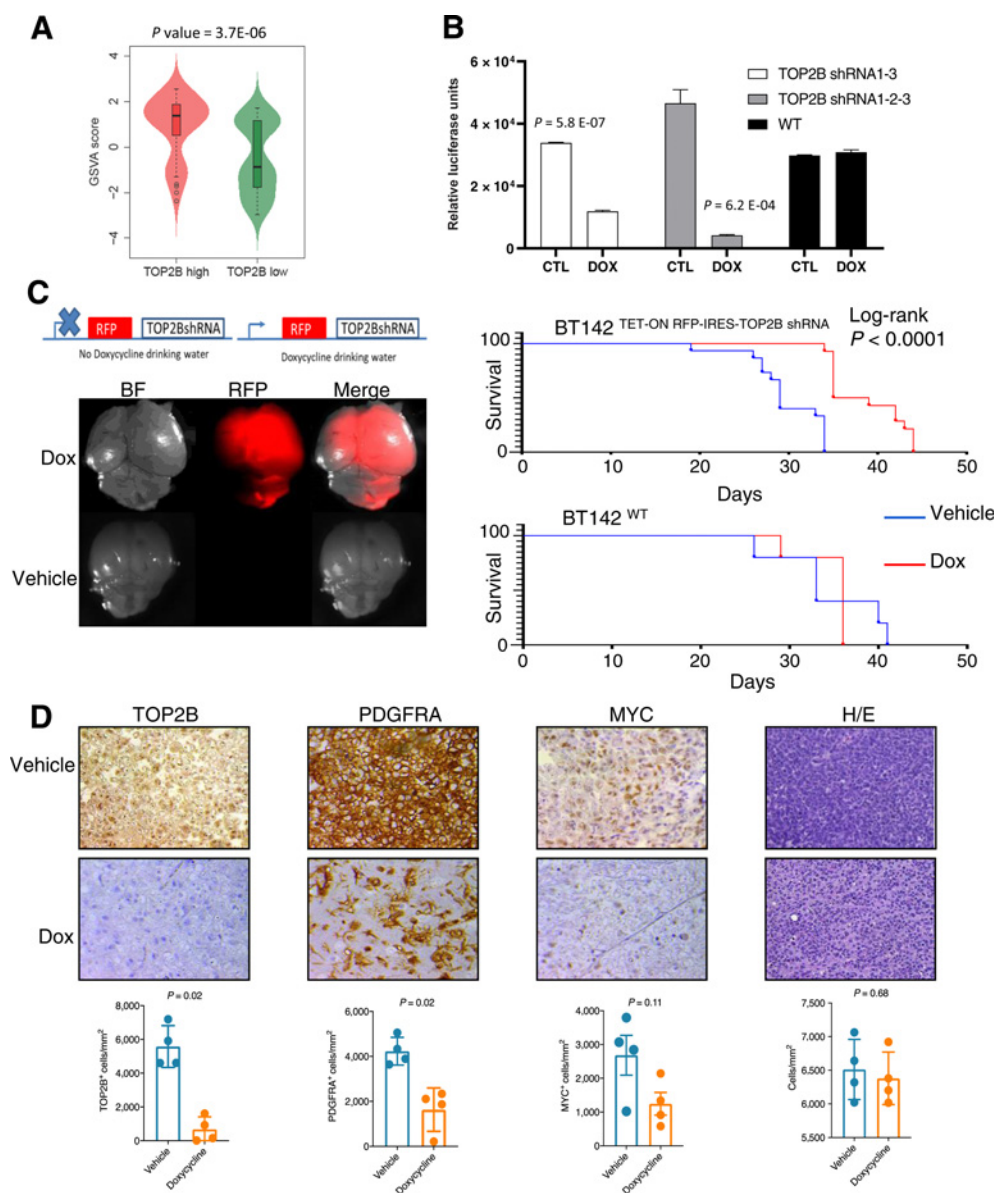

Figure 5.
TOP2B expression is associated with tumor growth phenotype in gliomas. **A,** Violin plot of GSVA analysis of genes related to cell-cycle genes comparing their expression on GBM specimens with high versus low TOP2B. **B,** Cell viability for TS543 glioma cells transduced with TET-ON inducible TOP2B shRNA treated with or without doxycycline, two representative clones are shown. Experiments were performed in five clones. **C,** Fluorescent microscopy and overall survival analysis following intracranial injection of BT142 TET-ON inducible TOP2B shRNA clones and treatment doxycycline or sucrose in drinking water (15 mice per group), and a similar survival analysis performed with BT142 untransduced cells (BT142^wt). **D,** IHC analysis for TOP2B, PDGFRA, MYC and, hematoxylin & eosin staining for cellular density using four mice bearing intracranial gliomas BT142 TET-ON with inducible TOP2B shRNA treated with or without doxycycline in the drinking water. Quantification for total TOP2B, PDGFRA, and MYC signal on entire tumors.

levels ($P = $ 3.7E-06, **Fig. 5A**). Moreover, we observed that TOP2 inhibition led to significant downregulation of the group of cancer genes that had TOP2B activity peaks (determined by etoposide-ChIP-seq) in both TS543 and BT142, but not of housekeeping genes with TOP2B activity peaks (refs. 36, 37; Supplementary Fig. S8). Given this, we hypothesized that TOP2B contributes to the proliferative/tumor growth phenotype of the subset of gliomas that express this topoisomerase.

To investigate the contribution of TOP2B to glioma growth, we silenced this gene in TS543 glioma cells and observed a significant decrease in cell viability (**Fig. 5B**). We next investigated the effects of TOP2B silencing *in vivo*. Intracranial implantation of BT142[TET-ON RFP-IRES-TOP2B shRNA] followed by administration of doxycycline in the drinking water led to intracranial glioma xenografts that exhibited RFP expression, but whose growth was impaired, as indicated by the significant prolongation in overall survival of doxycycline-treated mice, as compared with mice treated with sucrose (vehicle) in the drinking water. Yet, doxycycline in the drinking water did not lead to a difference in survival in case of mice implanted with untransduced BT142 cells (**Fig. 5C**). We analyzed the expression levels of TOP2B, PDGFRA, and MYC by IHC. As expected, doxycycline induced knockdown of TOP2B protein levels in intracranial glioma xenografts. We observed a significative PDGFRA downregulation ($P = 0.02$) consistent with the reduction of TOP2B. MYC protein levels showed a trend for downregulation following doxorubicin treatment ($P = 0.11$; **Fig. 5D**). Yet, we found that doxycycline treatment and TOP2B knockdown had no effect on overall cell density on these tumors (**Fig. 5D**).

Discussion

We showed that TOP2B promotes tumor growth in gliomas, and preferentially modulates the expression of multiple cancer genes, as opposed to housekeeping genes. In particular, we showed that TOP2B regulates the expression of oncogenes *PDGFRA* and *MYC* on these tumors, and contributes to the proliferative phenotype of a subset of gliomas. Several reports have implicated TOP2B in the regulation of transcription during development, and in physiologic conditions (10, 17, 19). Both TOP2A and TOP2B have also been implicated in gene rearrangements and translocations in cancer (13, 21, 38–40). We observed that TOP2B inhibition/silencing enhanced DNA damage response determined by γH2AX in glioma cell lines (Supplementary Fig. S9). Other groups previously demonstrated that TOP2B-induced DSB are important for transcription of *MYC*, and that pharmacologic TOP2 targeting downregulates this oncogene (31, 41, 42). Moreover, several reports have also attributed the cytotoxic effect of TOP2 poison doxorubicin on breast cancer cell lines to *MYC* downregulation (43–45). We show that *MYC* and a distant locus previously reported as a *MYC* enhancer region (34), exhibit TOP2B activity in gliomas that have elevated expression of this oncogene, consistent with the fact that the enzymatic reaction of TOP2B leads to DNA DSB. On the other hand, we show that TOP2B modulates the expression of *PDGFRA*. To our knowledge, our study is the first to implicate this enzyme in the transcriptional regulation of *PDGFRA*, and important oncogene for gliomas. We show that the effects of TOP2B on *PDGFRA* expression are occur both on tumors with amplification of this oncogene as well as in tumors that do not exhibit copy number changes for this growth factor receptor.

We have used malignant gliomas as a model for the transcriptional modulatory for TOP2B, though our results might prove generalizable

to other cancers. Variable expression of TOP2B has been previously reported (2, 46), but the consequences of this expression pattern were poorly understood. We provide experimental and correlative evidence supporting that TOP2B plays a role in regulation of specific genes on a subset of these tumors.

As opposed to previous reports exploring the study of TOP2B (9, 10, 13), we did not observe regulation of transcription by TOP2B to be associated with local maintenance of chromatin accessibility, as we did not detect changes at these regions with ATAC-seq at sites of TOP2B localization following it inhibition by ICRF-193. We also did not find TOP2B inhibition to have an effect on global DNA methylation (Supplementary Fig. S9). However, a subset of genes decorated with H3K27Ac and H3K4me3 histone marks showed a decrease in accessibility following inhibition with ICRF-193, but did not exhibit downregulation in this setting (see Supplementary Fig. S10). It is possible that the mechanism by which TOP2B regulates gene expression in gliomas may differ from that for neurons and stem cells, the systems where chromatin accessibility changes were described following ICRF-193 treatment (9, 10). Other differences between some of these reports and our investigation include the use of human cells, and the length of treatment with ICRF-193. It is possible that in gliomas TOP2B enzymatic inhibition led to changes in chromatin structure that are not captured by ATAC-seq, such as those that might take place by disruption of tridimensional chromatin interactions, such as the aberrant promoter-enhancer interaction responsible for *PDGFRA* expression on *IDH1*-mutant gliomas, and BT142 as previously described (3).

Previous groups have described that TOP2B can be poised on specific areas of the genome, and becomes enzymatically active when transcription at these sites is necessary (18). Moreover, etoposide has been utilized as a means of stabilizing TOP2–genome interactions for ChIP (29). By obtaining high-quality ChIP for native TOP2B, we were able to compare genomic loci for native TOP2B binding versus sites where TOP2B is enzymatically active. We discovered distinct locations for these types of interactions between TOP2B and the genome, as sites of TOP2B activity captured by etoposide ChIP do not always coincide with TOP2B native binding sites. Furthermore, our results show that regulation of gene expression by TOP2B occurs at promoters and introns where TOP2B is enzymatically active. Our observation of TOP2B enzymatic activity in the absence of binding in native conditions could be explained by tridimensional chromatin interactions. For example, recent work has revealed a close relationship between TOP2B and CTCF, a transcription factor that mediates inter and intra-chromosomal loops that are essential for enhancer–promoter interactions (14). Consistent with this, we also found the CTCF DNA binding motifs in the regions where TOP2B localized on the genome. The fact that we found a significant cooccurrence of TOP2B activity peaks (but not native binding peaks) with histone marks characteristic of enhancers such as H3K4me1 and H3K27Ac is consistent with tridimensional chromatin arrangements associated with promoter-enhancer interactions that could rely on TOP2B enzymatic activity. TOP2B involvement in mediating interactions between non-contiguous DNA sequences has also been suggested in association with the study of translocations and gene fusions that occur in other cancers (20, 21, 38–40, 47–49).

Our study provides evidence that TOP2B expression is associated with a proliferative phenotype. This is supported by the fact that TOP2B is associated with cell-cycle genes across human GBM, as well as the *in vitro* and *in vivo* evidence of impaired glioma cell growth upon silencing this enzyme.

The proliferative phenotype promoted by TOP2B, and the fact that this enzyme drives the expression of several oncogenes could lead to investigation of therapeutic targeting TOP2B as for a subset of gliomas.

Our study of TOP2B has several limitations that should be kept in mind. We relied on multiple glioma cell lines in which characterization of gene expression and ChIP-seq were performed *in vitro*. It is important to acknowledge that *in vitro* experiments could be influenced by artefacts and changes in tumor cell phenotype that relate to culture conditions. This limitation of our study was addressed by our complementary analysis of human glioma and brain tissues, and *in vivo* models. Another limitation is the use of TOP2 inhibitors for our TOP2B antagonism experiments, as these drugs can also target TOP2A, and thus contribution of TOP2A to the results obtained remains a possibility. Yet, we also present complementary gene silencing experiments that support that the regulation of transcription of PDGFRA and MYC can be specifically attributed to TOP2B.

Our study adds to a body of literature indicating that GBM is a complex disease, and that in spite of a shared histologic appearance there are many molecular differences across individual tumors. Here we provide evidence that a subset of these tumors rely on TOP2B activity for oncogene modulation and growth.

Authors' Disclosures

E. Gonzalez-Buendia reports grants from CONACYT during the conduct of the study and a patent for Therapeutic Modulation of Oncogenes by Pharmacologic TOP2 Targeting for Cancer pending. E. Feldstein reports a patent for WO2018094325A1 issued. J.N. Sarkaria reports grants from Basilea, Glaxo Smith Kline, Bristol Myers Squibb, Curtana, Forma, AbbVie, Actuate Boehringer Ingelheim, Celgene, Cible, Wayshine, Boston Scientific, AstraZeneca, Black Diamond, Karyopharm, and Bayer outside the submitted work. D.J. Brat reports grants from NCI during the conduct of the study. R. Rabadan reports other support from Genotwin and personal fees from Aimedbio outside the submitted work. No disclosures were reported by the other authors.

Authors' Contributions

E. Gonzalez-Buendia: Conceptualization, data curation, formal analysis, investigation, methodology, writing–original draft, project administration. **J. Zhao:** Data curation, software. **L. Wang:** Supervision, writing–review and editing. **S. Mukherjee:** Investigation. **D. Zhang:** Investigation. **V.A. Arrieta:** Investigation. **E. Feldstein:** Investigation. **J.R. Kane:** Investigation. **S. Kang:** Investigation. **C. Lee-Chang:** Investigation. **A. Mahajan:** Investigation. **L. Chen:** Investigation. **R. Realubit:** Resources, investigation. **C. Karan:** Resources, investigation. **L. Magnusson:** Investigation. **C. Horbinski:** Resources. **S.A. Marshall:** Investigation. **J.N. Sarkaria:** Resources. **A. Mohyeldin:** Resources. **I. Nakano:** Resources. **M. Bansal:** Investigation. **C.D. James:** Resources, writing–review and editing. **D.J. Brat:** Resources. **A. Ahmed:** Resources. **P. Canoll:** Resources. **R. Rabadan:** Resources, investigation, writing–review and editing. **A. Shilatifard:** Resources, supervision, writing–review and editing. **A.M. Sonabend:** Conceptualization, funding acquisition, methodology, writing–original draft, project administration.

References

1. Ceccarelli M, Barthel FP, Malta TM, Sabedot TS, Salama SR, Murray BA, et al. Molecular profiling reveals biologically discrete subsets and pathways of progression in diffuse glioma. Cell 2016;164:550–63.
2. Verhaak RGW, Hoadley KA, Purdom E, Wang V, Qi Y, Wilkerson MD, et al. Integrated genomic analysis identifies clinically relevant subtypes of glioblastoma characterized by abnormalities in PDGFRA, IDH1, EGFR, and NF1. Cancer Cell 2010;17:98–110.
3. Flavahan WA, Drier Y, Liau BB, Gillespie SM, Venteicher AS, Stemmer-Rachamimov AO, et al. Insulator dysfunction and oncogene activation in IDH mutant gliomas. Nature 2016;529:110.
4. Turcan S, Rohle D, Goenka A, Walsh LA, Fang F, Yilmaz E, et al. IDH1 mutation is sufficient to establish the glioma hypermethylator phenotype. Nature 2012;483:479.
5. Dang L, White DW, Gross S, Bennett BD, Bittinger MA, Driggers EM, et al. Cancer-associated IDH1 mutations produce 2-hydroxyglutarate. Nature 2010;465:966.
6. Yan H, Parsons DW, Jin G, McLendon R, Rasheed BA, Yuan W, et al. IDH1 and IDH2 mutations in gliomas. N Engl J Med 2009;360:765–73.
7. Piunti A, Hashizume R, Morgan MA, Bartom ET, Horbinski CM, Marshall SA, et al. Therapeutic targeting of polycomb and BET bromodomain proteins in diffuse intrinsic pontine gliomas. Nat Med 2017;23:493–500.
8. Schwartzentruber J, Korshunov A, Liu X-Y, Jones DTW, Pfaff E, Jacob K, et al. Driver mutations in histone H3.3 and chromatin remodelling genes in paediatric glioblastoma. Nature 2012;482:226–31.
9. Thakurela S, Garding A, Jung J, Schübeler D, Burger L, Tiwari VK. Gene regulation and priming by topoisomerase IIalpha in embryonic stem cells. Nat Commun 2013;4:2478.
10. Tiwari VK, Burger L, Nikoletopoulou V, Deogracias R, Thakurela S, Wirbelauer C, et al. Target genes of Topoisomerase IIbeta regulate neuronal survival and are defined by their chromatin state. Proc Natl Acad Sci U S A 2012;109:E934–43.
11. Mirkovitch J, Gasser SM, Laemmli UK. Relation of chromosome structure and gene expression. Philos Trans R Soc Lond B Biol Sci 1987;317:563–74.
12. Adachi Y, Käs E, Laemmli UK. Preferential, cooperative binding of DNA topoisomerase II to scaffold-associated regions. EMBO J 1989;8:3997–4006.
13. Canela A, Maman Y, Jung S, Wong N, Callen E, Day A, et al. Genome organization drives chromosome fragility. Cell 2017;170:507–21.
14. Uusküla-Reimand L, Hou H, Samavarchi-Tehrani P, Rudan MV, Liang M, Medina-Rivera A, et al. Topoisomerase II beta interacts with cohesin and CTCF at topological domain borders. Genome Biol 2016;17:182.
15. Pommier Y, Sun Y, Huang S-Y, Nitiss JL. Roles of eukaryotic topoisomerases in transcription, replication and genomic stability. Nat Rev Mol Cell Biol 2016;17:703.
16. Nitiss JL. DNA topoisomerase II and its growing repertoire of biological functions. Nat Rev Cancer 2009;9:327–37.
17. Nevin LM, Xiao T, Staub W, Baier H. Topoisomerase IIbeta is required for lamina-specific targeting of retinal ganglion cell axons and dendrites. Development 2011;138:2457–65.
18. Madabhushi R, Gao F, Pfenning AR, Pan L, Yamakawa S, Seo J, et al. Activity-induced DNA breaks govern the expression of neuronal early-response genes. Cell 2015;161:1592–605.
19. King IF, Yandava CN, Mabb AM, Hsiao JS, Huang H-S, Pearson BL, et al. Topoisomerases facilitate transcription of long genes linked to autism. Nature 2013;501:58–62.
20. Cowell IG, Sondka Z, Smith K, Lee KC, Manville CM, Sidorczuk-Lesthuruge M, et al. Model for MLL translocations in therapy-related leukemia involving topoisomerase IIβ-mediated DNA strand breaks and gene proximity. Proceedings of the National Academy of Sciences U S A 2012;109:8989–94.

21. Haffner MC, Aryee MJ, Toubaji A, Esopi DM, Albadine R, Gurel B, et al. Androgen-induced TOP2B-mediated double-strand breaks and prostate cancer gene rearrangements. Nat Genet 2010;42:668.

22. Szerlip NJ, Pedraza A, Chakravarty D, Azim M, McGuire J, Fang Y, et al. Intratumoral heterogeneity of receptor tyrosine kinases EGFR and PDGFRA amplification in glioblastoma defines subpopulations with distinct growth factor response. Proc Natl Acad Sci 2012;109:3041–6.

23. Buenrostro JD, Wu B, Chang HY, Greenleaf WJ. ATAC-seq: a method for assaying chromatin accessibility genome-wide. Curr Protoc Mol Biol. 2015;109: 21.29.1–21.29.9.

24. Sano K, Miyaji-Yamaguchi M, Tsutsui KM, Tsutsui K. Topoisomerase IIβ activates a subset of neuronal genes that are repressed in AT-rich genomic environment. PLoS One 2008;3:e4103.

25. Quinlan AR, Hall IM. BEDTools: a flexible suite of utilities for comparing genomic features. Bioinformatics 2010;26:841–2.

26. Kane JR, Zhao J, Tsujiuchi T, Laffleur B, Arrieta VA, Mahajan A, et al. CD8$^+$ T-cell–mediated immunoediting influences genomic evolution and immune evasion in murine gliomas. Clin Cancer Res 2020;26:4390.

27. Tewey KM, Rowe TC, Yang L, Halligan BD, Liu LF. Adriamycin-induced DNA damage mediated by mammalian DNA topoisomerase II. Science 1984;226:466.

28. Nitiss JL. Targeting DNA topoisomerase II in cancer chemotherapy. Nat Rev Cancer 2009;9:338–50.

29. Miller EL, Hargreaves DC, Kadoch C, Chang C-Y, Calarco JP, Hodges C, et al. TOP2 synergizes with BAF chromatin remodeling for both resolution and formation of facultative heterochromatin. Nat Struct Mol Biol 2017;24:344–52.

30. Tanabe K, Ikegami Y, Ishida R, Andoh T. Inhibition of topoisomerase II by antitumor agents Bis(2,6-dioxopiperazine) derivatives. Cancer Res 1991;51: 4903–8.

31. Bunch H, Lawney BP, Lin Y-F, Asaithamby A, Murshid A, Wang YE, et al. Transcriptional elongation requires DNA break-induced signalling. Nat Commun 2015;6:10191.

32. Liberzon A, Subramanian A, Pinchback R, Thorvaldsdottir H, Tamayo P, Mesirov JP. Molecular signatures database (MSigDB) 3.0. Bioinformatics 2011;27:1739–40.

33. Subramanian A, Tamayo P, Mootha VK, Mukherjee S, Ebert BL, Gillette MA, et al. Gene set enrichment analysis: A knowledge-based approach for interpreting genome-wide expression profiles. Proc Natl Acad Sci U S A 2005;102:15545.

34. Herranz D, Ambesi-Impiombato A, Palomero T, Schnell SA, Belver L, Wendorff AA, et al. A NOTCH1-driven MYC enhancer promotes T cell development, transformation and acute lymphoblastic leukemia. Nat Med 2014;20:1130.

35. Brennan CW, Verhaak RGW, McKenna A, Campos B, Noushmehr H, Salama SR, et al. The somatic genomic landscape of glioblastoma. Cell 2013;155:462–77.

36. Futreal PA, Coin L, Marshall M, Down T, Hubbard T, Wooster R, et al. A census of human cancer genes. Nat Rev Cancer 2004;4:177–83.

37. Eisenberg E, Levanon EY. Human housekeeping genes, revisited. Trends Genet 2013;29:569–74.

38. Felix CA, Kolaris CP, Osheroff N. Topoisomerase II and the etiology of chromosomal translocations. DNA Repair (Amst) 2006;5:1093–108.

39. Yu X, Davenport JW, Urtishak KA, Carillo ML, Gosai SJ, Kolaris CP, et al. Genome-wide TOP2A DNA cleavage is biased toward translocated and highly transcribed loci. Genome Res 2017;27:1238–49.

40. Canela A, Maman Y, Huang S-YN, Wutz G, Tang W, Zagnoli-Vieira G, et al. Topoisomerase II-induced chromosome breakage and translocation is determined by chromosome architecture and transcriptional activity. Mol Cell 2019; 75:252–68,.

41. Riou J-F, Multon E, Vilarem M-J, Larsen C-J, Riou G. In vivo stimulation by antitumor drugs of the topoisomerase II induced cleavage sites in c-myc protooncogene. Biochem Biophys Res Commun 1986;137:154–60.

42. Pommier Y, Orr A, Kohn KW, Riou J-F. Differential effects of amsacrine and epipodophyllotoxins on topoisomerase II cleavage in the human c-myc proto-oncogene. Cancer Res 1992;52:3125–30.

43. Lu H-R, Meng L-H, Huang M, Zhu H, Miao Z-H, Ding J. DNA damage, c-myc suppression and apoptosis induced by the novel topoisomerase II inhibitor, salvicine, in human breast cancer MCF-7 cells. Cancer Chemother Pharmacol 2005;55:286–94.

44. Bunch RT, Povirk LF, Orr MS, Randolph JK, Fornari FA, Gewirtz DA. Influence of amsacrine (m-AMSA) on bulk and gene-specific DNA damage and c-myc expression in MCF-7 breast tumor cells. Biochem Pharmacol 1994;47:317–29.

45. Fornari FA, Jarvis WD, Grant S, Orr MS, Randolph JK, White FKH, et al. Growth arrest and non-apoptotic cell death associated with the suppression of c-myc Expression in MCF-7 breast tumor cells following acute exposure to doxorubicin. Biochem Pharmacol 1996;51:931–40.

46. Sonabend AM, Carminucci AS, Amendolara B, Bansal M, Leung R, Lei L, et al. Convection-enhanced delivery of etoposide is effective against murine proneural glioblastoma. Neuro Oncol 2014;16:1210–9.

47. Super H, McCabe N, Thirman M, Larson R, Le Beau M, Pedersen-Bjergaard J, et al. Rearrangements of the MLL gene in therapy-related acute myeloid leukemia in patients previously treated with agents targeting DNA- topoisomerase II. Blood 1993;82:3705–11.

48. Metzler M, Staege MS, Harder L, Mendelova D, Zuna J, Fronkova E, et al. Inv(11)(q21q23) fuses MLL to the Notch co-activator mastermind-like 2 in secondary T-cell acute lymphoblastic leukemia. Leukemia 2008; 22:1807.

49. Gothe HJ, Bouwman BAM, Gusmao EG, Piccinno R, Petrosino G, Sayols S, et al. Spatial chromosome folding and active transcription drive DNA fragility and formation of oncogenic MLL translocations. Mol Cell 2019; 75:267–83.